Food and Chemical Toxicology 69 (2014) 202–209

Contents lists available at ScienceDirect

Food and Chemical Toxicology

journal homepage: www.elsevier.com/locate/foodchemtox

Central role of Nix in the autophagic response to ochratoxin A

Xiao Li Shen [a,b,1], Boyang Zhang [a,1], Rui Liang [a], Wen-Hsing Cheng [c], Wentao Xu [a,*], YunBo Luo [a], Changhui Zhao [d], Kunlun Huang [a]

[a] Laboratory of Food Safety and Molecular Biology, College of Food Science and Nutritional Engineering, China Agricultural University, Beijing 100083, PR China
[b] School of Public Health, Zunyi Medical University, Zunyi, Guizhou 563003, PR China
[c] Department of Food Science, Nutrition and Health Promotion, Mississippi State University, MS 39762, USA
[d] Department of Nutrition and Food Science, University of Maryland, College Park, MD 20742, USA

ARTICLE INFO

Article history:
Received 18 January 2014
Accepted 8 April 2014
Available online 19 April 2014

Keywords:
Ochratoxin A
Autophagy
Mitophagy
Apoptosis
Renal cytotoxicity

ABSTRACT

Nephrotoxicity is the most prominent toxicological effects of ochratoxin A (OTA). We have previously shown that autophagy might be involved in OTA-induced early renal cytotoxicity, but the mechanisms of action are unknown. Since OTA is known to induce mitochondrial damage and Nix is a selective autophagy receptor for mitochondrial clearance, the objective of this study was to investigate whether Nix mediates autophagic response to OTA-induced renal cytotoxicity. Our results showed that OTA induced autophagic and mitophagic activitits. *Nix* shRNA HEK 293 cells were more sensitive than scrambled shRNA cells to OTA-induced cell death, and differentially affect the mRNA expression of *SDHA*, *AIFM1*, and *Bad* and protein expression of AIF, VDAC, SDHA and LONP1 after OTA treatment. In particular, up-regulation of the pro-apoptotic *Bad* and AIF after OTA treatment was prominent only in *Nix* shRNA cells, which might explain the higher ratio of cell death. These results might indicate that Nix plays a critical role in the cellular protection against OTA toxicity through autophagy and mitochondria.

1. Introduction

The mycotoxin ochratoxin A (OTA) was first discovered as a fungal metabolite of *Aspergillus ochraceus* Wilh in 1965 (van der Merwe et al., 1965). OTA has been implicated in a diverse range of toxicological effects, including carcinogenicity, teratogenicity, mutagenicity, genotoxicity, immunotoxicity, neurotoxicity, nephrotoxicity and hepatotoxicity (Liu et al., 2012; Marin-Kuan et al., 2006; O'Brien and Dietrich, 2005). Kidney is the main target organ of OTA (Lühe et al., 2003). OTA is considered as a major causal determinant of mycotoxic porcine nephropathy as well as endemic Balkan nephropathy in humans (Hald, 1991; Stoev, 1998). Both diseases are characterized by degenerative changes in the epithelial cells of the proximal tubules and proliferative changes in the interstitium and changes in various haematological and biochemical parameters (Stoev et al., 2001). Because of its wide presence in a variety of foodstuffs, including cereals (corn, wheat, barley, oats, rye), beans, pork, eggs, fish, poultry, milk, cheese, dried fruits, wine, beer, tea, coffee, cocoa and herbs (Bhatnagar et al., 2002), humans are at a high risk of being continuously exposed to OTA. More importantly, OTA is a persistent toxin with a blood half-life up to 853.2 h in humans (Studer-Rohr et al., 2000). Thus, OTA remains a dietary toxicant of global concern (Duarte et al., 2010).

Mitochondrial dysfunction is an early event during the development of OTA toxicity (Aleo et al., 1991). Interestingly, autophagy that occurs in mitochondria (also known as "mitophagy") has been reported to protect against oxidative stress and mitochondrial dysfunction (Lemasters, 2005). Autophagy is a self-destruction system conserved among eukaryotes, in which cytoplasmic components including organelles are entrapped into a double membrane structure called the autophagosome and followed by fused with lysosome to form an autolysosome, followed by degradation of the captured cytoplasmic components by lysosomal hydrolases (Komatsu and Ichimura, 2010). Consequently, autophagy or mitophagy in principal serves an adaptive role to protect organisms against diverse pathologies, including infections, inflammatory diseases, heart disease (Levine and Kroemer, 2008), neurodegeneration (Gusdon and Chu, 2011; Vives-Bauza and Przedborski, 2011), aging (Batlevi and La Spada, 2011) and cancer (Jin, 2006; Levine and Kroemer, 2008). However, to our knowledge, no study has concerned whether autophagy or mitophagy plays an important role in the pathogenesis of OTA-induced renal diseases.

Recent reports indicate that mitochondria are recognized for selective mitophagy either by PINK1 and Parkin or mitophagic

* Corresponding author. Tel./fax: +86 10 6273 7786.
E-mail address: xuwentao@cau.edu.cn (W. Xu).
[1] These authors contributed equally.

http://dx.doi.org/10.1016/j.fct.2014.04.017
0278-6915/

receptors Bcl2-related protein Nix (Bnip3L) and Bnip3 and their accompanying modulators. PINK1/Parkin-mediated mitophagy mediates the cargo recognition function through polyubiquitination of mitochondrial proteins, while Nix functions as a regulated mitophagy receptor (Novak, 2012). Novak et al. (2010) reported that Nix is a mitochondrial outer membrane protein and mediates mitochondrial clearance after mitochondrial damage during erythrocyte differentiation (Kanki, 2010; Schweers et al., 2007). Nonetheless, whether Nix plays a crucial role in the pathogenesis of OTA-induced renal cytotoxicity remains to be clarified. Therefore, *Nix* RNA interference (RNAi) was employed to determine the role of autophagy or mitophagy in OTA-induced renal cytotoxicity.

2. Materials and methods

2.1. Plasmids construction

To generate enhanced green fluorescent protein (EGFP)-LC3B fusion DNA fragment, EGFP and LC3B were amplified by PCR using the plasmid pLL3.7 and human cDNA as the template, respectively. The sequences of primer were as follows: EGFP, 5′-CGTGTACGGTGGGAGGTCTA-3′ (forward) and 5′-GGTCTTCTCCGACGGCATCTTGTACAGCTCGTCCATGC-3′ (reverse); LC3B, 5′-ATGCCGTCGGAGAAGACC-3′ (forward) and 5′-ATCGAATTCTTACACTGACAATTTCATCCCG-3′ (reverse). The resulting PCR products of EGFP and LC3B were purified by Gel Extraction Kit (cwbiotech, Beijing, PRC) and then used as the template of secondary overlap PCR. The forward primer of EGFP and the reverse primer of LC3B were used for overlap PCR. The resulting amplified fusion product was cloned into the *Nhe*I and *Eco*RI sites of pLL3.7 to produce pLL3.7-EGFP-LC3B. All constructs were verified by DNA sequencing.

To generate *Nix* small hairpin RNA (shRNA), the double-stranded oligonucleotides targeting *Nix* gene were cloned into *Xho*I-digested and *Hpa*I-digested pLentiLox3.7 (pLL3.7). The sequence of the oligonucleotides was 5′-TGCAATGCTATTATCTCTAATCAAGAGTTAGAGATAATAGCATTGCTTTTTTC-3′ (forward) and 5′-TCGAGAAAAAAGCAATGCTATTATCTCTAACTCTTGATTAGAGATAATAGCATTGCA-3′ (reverse). The scrambled (control) shRNA sequence was 5′-TGTCAACTCATGTATTACTATCAAGAGTAGTAATACATGAGTTGACTTTTTTC-3′ (forward) and 5′-TCGAGAAAAAAGTCAACTCATGTATTACTACTCTTGATAGTAATACATGAGTTGACA-3′ (reverse).

2.2. Cell culture, transfection and treatment

Human Embryonic Kidney 293 (HEK 293) cells (our laboratory) were cultured in Dulbecco's modified Eagle's medium (DMEM) (Macgene, Beijing, PRC) containing 10% fetal bovine serum (FBS) (Hyclone, Beijing, PRC), 100 U/mL penicillin, 100 μg/mL streptomycin, 250 ng/ml amphotericin B (Macgene, PRC), 2 mM L-glutamine (Sigma, Beijing, PRC), and 1% MEM Nonessential Amino Acids (Macgene, Beijing, PRC) in 95% saturated humidity and 5% CO_2 atmosphere at 37 °C (Shen et al., 2013).

Lentiviral vector pLL3.7-*Nix*-shRNA along with the packaging plasmids (pCMV-VSV-G, pRSV-Rev and pMDLg/pRRE) were mixed together and transfected into the adherent HEK 293 cells according to the manual of VigoFect (Vigorous, Beijing, PRC). The pLL3.7 plasmid with scrambled sequence of *Nix* was uniformly cotransfected with package plasmids as a control. Culture supernatants containing lentiviruses were collected 30 h after transfection and were used to infect a new batch of HEK 293 cells. The resulting HEK 293 cells were divided into two experimental groups: RNAi group and control group. Each group was treated with 0, 1, 5, 10, 20, 50, 100 μM OTA (Fermentek, Beijing, PRC) for 5 h.

The transfection of pLL3.7-EGFP-LC3B was the same as pLL3.7-*Nix*-shRNA. The transfected HEK 293 cells were treated with 0 and 20 μM OTA for 2 h (Shen et al., 2013).

2.3. Cell viability assay

Cell Counting Kit-8 (WST-8, Beyotime, Jiangsu, PRC) is superior to MTT assay for analyzing cell proliferation and toxicity, because it can be reduced to soluble formazan by dehydrogenase in mitochondria and has little toxicity to cells. According to manufacturer's instructions, 1×10^4 cells/well were seeded in a 96-well flat-bottomed plate, grown at 37 °C for 24 h, treated at the indicated concentration of OTA, and washed once with phosphate-buffered saline (PBS). Subsequently, 10 μl of WST-8 dye and 100 μl of PBS were added to each well, and cells were incubated at 37 °C for 3 h. Finally, dye absorbance was determined at 450 nm using a plate reader (Thermo Scientific, USA) (Shen et al., 2013).

2.4. Image analyses by confocal microscopy

For autophagy imaging experiments, EGFP-LC3B transfected HEK 293 cells were grown at 37 °C on MatTek glass bottom culture dishes. Images of samples were observed under a Leica TCS SP5 confocal laser scanning microscope (Leica, Germany) with 630× magnification. Maximum projected images from each Z series were used for quantification of LC3B dots. A minimum of 15 randomly selected cells from three independent experiments were analyzed (Lim et al., 2011).

For mitophagy imaging experiments, HEK 293 cells were grown at 37 °C on MatTek glass bottom culture dishes and were divided into four experimental groups: treated with serum-free medium for 2 h as a control (group CK); pretreated with 10 μM chloroquine diphosphate salt (CQ, a lysosomal inhibitor that prevents fusion between autophagosomes and lysosomes by raising the lysosomal pH (Ding et al., 2010; Lim et al., 2011)) (Sigma) for 2 h (group CK-CQ), treated with 20 μM OTA for 2 h (group O); pretreated with 10 μM CQ for 2 h and then treated with 20 μM OTA for 2 h (group O-CQ). Subsequently, cells were washed twice with PBS, and then were loaded with fluorophores Mito-Tracker Green (MTG, 0.5 μM) and Lyso-Tracker Red (LTR, 0.5 μM) (Beyotime, PRC) for 1 h to locate mitochondria and lysosomes, respectively (Rodriguez-Enriquez et al., 2006). After that, cells were observed by confocal microscopy as described above and the number of yellow fluorescence dots was quantified.

2.5. RNA extraction and qRT-PCR

RNA extraction, cDNA synthesis and quantitative reverse transcriptase-polymerase chain reaction (qRT-PCR) were performed as previously described (Shen et al., 2013). Gene specific primers for each of the target genes were designed by NCBI Primer-BLAST. The sequences of primer were shown in Table 1.

2.6. Western blot analysis

The cells were lysed on ice in RIPA lysis buffer containing 50 mM Tris–HCl pH 7.4, 150 mM NaCl, 1% sodium deoxycholate, 1% Triton X-100, 0.1% SDS and complete protease inhibitor cocktail (EDTA, sodium orthovanadate, sodium fluoride, leupeptin) (Beyotime, Jiangsu, PRC) supplemented with 1 mM PMSF. Cells were then homogenized by using a 1 ml syringe (Lim et al., 2011). Cell lysates were centrifuged at 13,000*g* for 10 min at 4 °C. The supernatant was collected and total proteins quantified using BCA Protein Assay Kit (Cwbiotech, Beijing, PRC). Proteins (40 μg/lane) were loaded, separated on 4–13% gradual SDS-PAGE gels. The separated protein bands were transferred onto nitrocellulose membranes under 80 V for 1.5 h in ice. Nonspecific binding was blocked by incubating the membranes in blocking buffer (1% BAS and Tris-buffered saline containing 0.1% Tween-20 (TBST)) for 1 h. Then, membranes were incubated for 1 h with one of the following primary antibodies: rabbit anti-VDAC (Cell Signaling, 4661; 1:1000), rabbit anti-AIF (Cell Signaling, 5318; 1:1000), rabbit anti-SDHA (Cell Signaling, 5839; 1:1000), rabbit anti-LONP1 (Proteintech, 15440-1-AP; 1:1000), rabbit anti-LC3B (Cell Signaling, 3868; 1:1000) and rabbit anti-β-Actin (Cell Signaling, 4970; 1:1000). After washing the membranes with TBST for 3 times and 5 min for each time, membranes were incubated with AP-labeled goat anti-rabbit (Beyotime, Jiangsu, PRC). After washing 3 times with PBS, specific bands were detected using BCIP/NBT (Merck-Calbiochem Beijing, PRC). Total gray values of each band were digitized by using BandScan V4.3. The relative expression level of each protein was normalized using β-Actin as reference, and the protein expression in the untreated scrambled cells (S0) was defined as 1 (Shen et al., 2013).

2.7. Statistical analysis

Microsoft Excel 2003 and SPSS 13.0 were used for the statistical analysis. Data were subjected to analysis of variance (ANOVA) and multiple comparisons using Duncan. Differences were considered to be significant with $p < 0.05$ (Shen et al., 2010).

3. Results

3.1. Autophagy analysis

LC3B is a general marker for autophagic membranes during the maturation of autophagosome. This process can be examined by

Table 1
Gene specific primers used in qRT-PCR analysis.

Gene name	Forward primer	Reverse primer
Bax	AACTGGACAGTAACATGGA	CTGGCAAAGTAGAAAAGG
Bcl-2	GTCATGTGTGTGGAGAGC	CAGGAGAAATCAAACAGAG
Bcl-X_L	GACAAGGAGATGCAGGTATT	CCATAGAGTTCCACAAAAGTAT
Bid	GCTGTAAACTTCCAATTTCT	GTTTTGACTGTCCCTAAGAG
Bad	GAGGATGAGTGACGAGTTT	CACCAGGACTGGAAGAC
Caspase-3	CTCCTTCCATCAAATAGAAC	AATTAACAATCATTGCCTCT
Caspase-8	TGTCTCCTTTCTCTTATGCT	ACAGTGGGCTTATAGTTGAT
Caspase-9	TAGAAAACCTTACCCCAGT	ATTGTTGATAATGAGGCAGT
AIFM1	GTGATTCAACTCTTCCCCGA	ACTGCTGACTCCAACGGATT
Nix	CCACCAGACTAGACCTGTAT	CTCAAACTTAGGGAAACTTG

visualizing the EGFP-LC3B fusing protein expression and structure under a high-resolution fluorescence microscope (Mizushima, 2004). The over-expression of EGFP-LC3B does not affect endogenous autophagy (Mizushima et al., 2004). We observed that the different developmental stage of autophagosome (Fig. 1A, arrows 1–4). Compared with the control, EGFP-LC3B patches were significantly increased with the treatment of OTA (Fig. 1A and B). This indicates that the treatment of OTA induces autophagosome formation.

3.2. Mitophagy analysis

In the absence of OTA or CQ treatment (the CK group), only a little mitochondria co-localize with lysosome (Fig. 2). After treating the HEK293 cells with OTA (the O group), mitophagic activity was increased to some degree, as evidenced by the yellow fluorescence. Because autophagosomes are degraded when fuse to lysosomes, we added CQ to prevent autophagosome degradation to better assess mitophagic flux that reflects accumulative mitophagic activity. Compared with control, the treatment of OTA induced mitophagic flux activity increase (Fig. 2). It revealed that the treatment of OTA increased mitophagy. This confirmed our previous hypothesis that the treatment of OTA involved in induction of autophagy and mitophagy (Shen et al., 2013).

3.3. Cell viability analysis

The relative mRNA expression of *Nix* was decreased by 87.9% via *Nix* shRNA (Fig. 3). Both Nix shRNA and scrambled shRNA HEK 293 cells showed an OTA dose-dependent effect on the killing of HEK 293 cells (0–100 μM); however, Nix shRNA HEK 293 cells were more sensitive than scrambled shRNA HEK 293 cells to OTA treatment (Fig. 4). These results suggest an important role of *Nix* in protection against OTA-induced cytotoxicity. When the OTA concentration was elevated to 10 μM, the cell death rate in both *Nix* cells and the scrambled became significant. Therefore, we chose 10 μM OTA for further experiment.

3.4. qRT-PCR analysis

Next, we determined the mRNA expression in the apoptosis pathway by qRT-PCR. We chose an OTA concentration at 10 μM because this dosage killed about 10% of the cells and has been shown to induce mitochondrial damage and dysfunction (Shen et al., 2013). As shown in Fig. 5, the mRNA expression of *caspase-3*, *caspase-8*, *Bcl-2*, *Bcl-X_L* and *Bid* were decreased by at least 60% after OTA treatment in both Nix and scrambled shRNA cells (N10 and S10), and their expression did not differ between Nix and scrambled shRNA cells before (N0 and S0) or after (N10 and S10) OTA treatment. The OTA treatment also suppressed the mRNA expression of *SDHA* and *AIFM1* in both Nix and scrambled shRNA cells, but their expression were lower in Nix than in scrambled shRNA cells after the OTA treatment. *Caspase-9* mRNA level was greater in Nix than in scrambled shRNA cells before or after OTA treatment, and was lower after OTA treatment in Nix but not scrambled shRNA cells. *Bax* mRNA level did not differ by Nix shRNA knockdown, although the expression was slightly decreased after OTA treatment in both Nix and scrambled shRNA cells. Interestingly, *Bad* mRNA expression was induced by OTA treatment only in Nix shRNA cells such that the level was greater in Nix than in scrambled shRNA cells after OTA treatment.

In a word, *Nix* knockdown did not affect the expression of *caspase-3*, *SDHA*, *AIFM1*, *Bax*, *Bcl-2*, *Bcl-X_L*, *Bid* and *Bad*, but indeed made some genes (*SDHA*, *AIFM1*, and *Bad*) more sensitive to OTA.

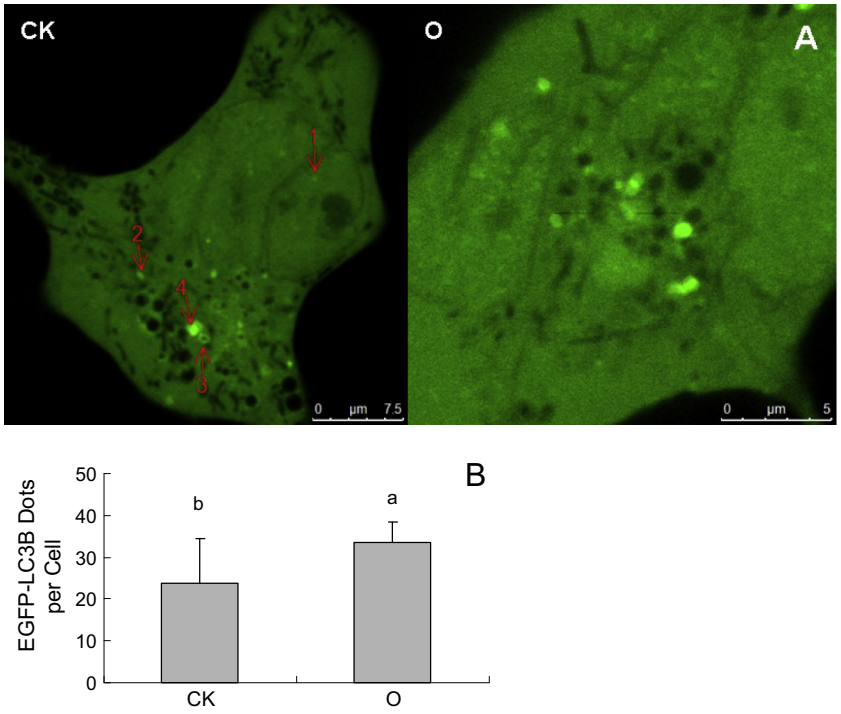

Fig. 1. Autophagy was evident with the treatment of OTA. EGFP-LC3B transfected HEK 293 cells were treated with 20 μM OTA for 2 h (group O) or with serum-free medium as a control (group CK). (A) Arrows illustrate the development of autophagosomes: small EGFP-LC3B dot [pre-autophagosomal structure (PAS, arrow 1)]; PAS progressed in EGFP-LC3B crescent structure to form isolation membrane/phagophore (arrow 2); followed by EGFP-LC3B ring structure (early autophagosome, arrow 3); then formed bright EGFP-LC3B spherical structure (late autophagosome, arrow 4). (B) The number of autophagosomes per cell was counted. Different lowercase letters indicate significant differences ($p < 0.05$). Data were shown in mean ± SD ($n = 15$).

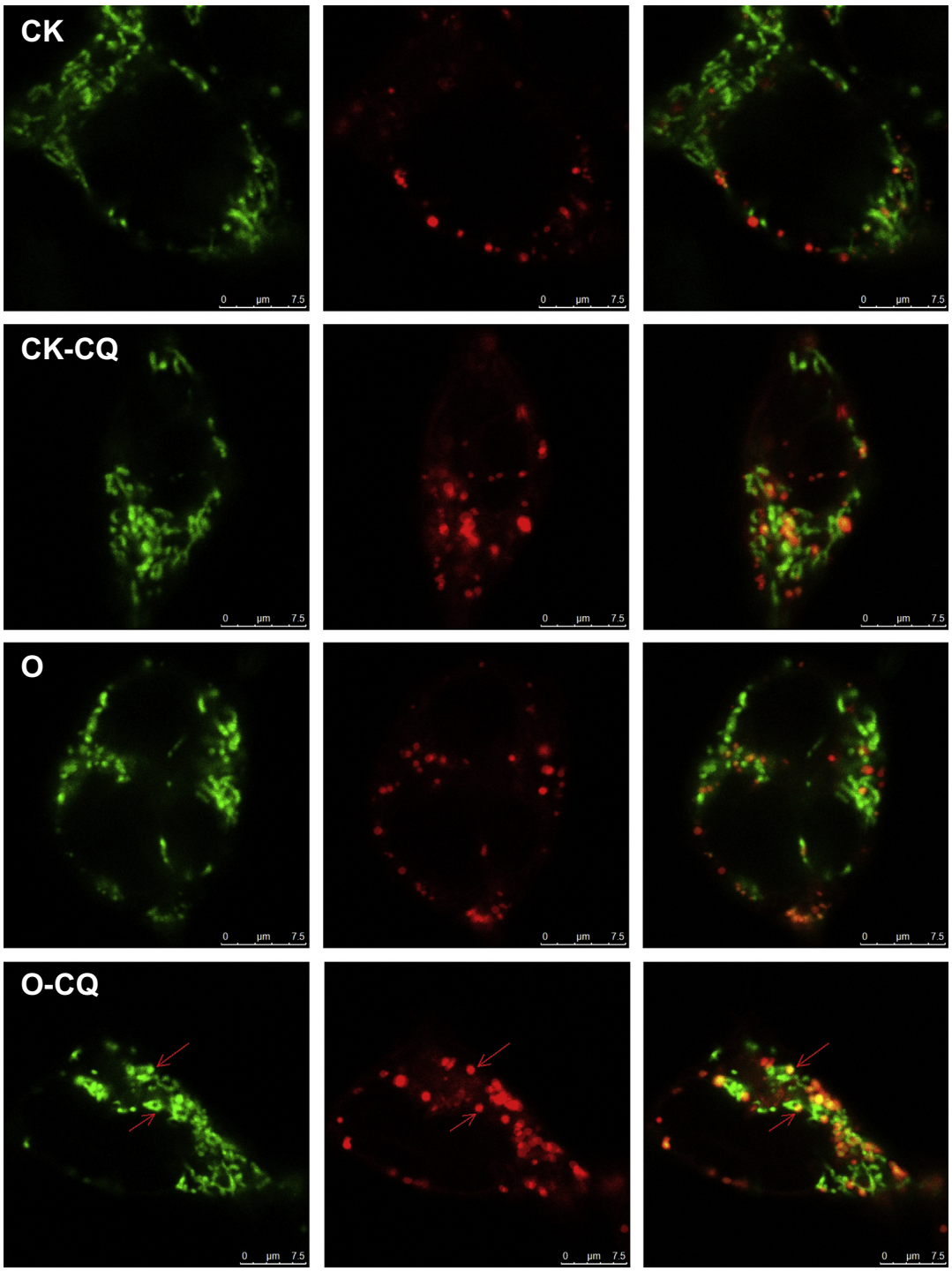

Fig. 2. Mitophagy was increased with the treatment of OTA. HEK 293 cells were treated with (1) serum-free medium only (group CK); (2) 10 μM chloroquine diphosphate salt (CQ) for 2 h (group CK-CQ); (3) 20 μM OTA for 2 h (group O) and (4) 10 μM CQ for 2 h followed by treatment with 20 μM OTA for 2 h (group O-CQ). Mitochondria were located by green-fluorescing Mito-Tracker Green (left), lysosomes were located by red-fluorescing Lyso-Tracker Red (middle), and the yellow fluorescence represents co-localization between mitochondria and lysosome, an indicator of mitophagy (right). Representative pictures were shown. (For interpretation of the references to color in this figure legend, the reader is referred to the web version of this article.)

3.5. Western blot analysis

As shown in Fig. 6, OTA treatment decreased the protein expression of SDHA but not AIF, VDAC or LONP1 in scrambled shRNA cells. In contrast, OTA treatment increased the expression of all the proteins in Nix shRNA cells. Nix knockdown increased the protein expression of AIF but decreased the expression of VDAC and LONP1 in the absence of OTA treatment. After OTA treatment, Nix knockdown resulted in an increased protein expression of AIF, VDAC and SDHA, but not LONP1.

As shown in Fig. 7, knockdown of *Nix* expression resulted in a decrease in autophagic activity before or after OTA treatment, as evidenced by the ratio of LC3BII/LC3BI. Interestingly, the OTA-induced autophagic activity was shown in scrambled but not nix

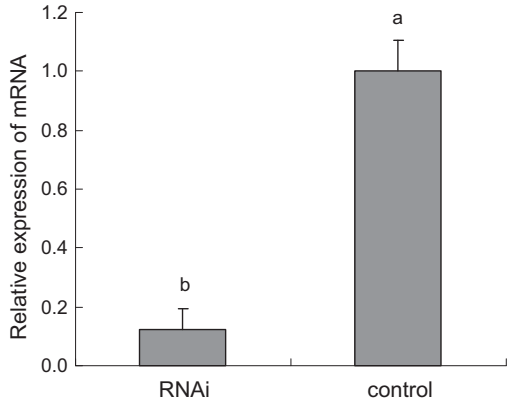

Fig. 3. The efficacy of *Nix* and scrambled shRNA on the expression of *Nix* mRNA in HEK293 cells. Different lowercase letters indicate significant differences ($p < 0.05$). Data were shown in mean ± SD ($n = 3$).

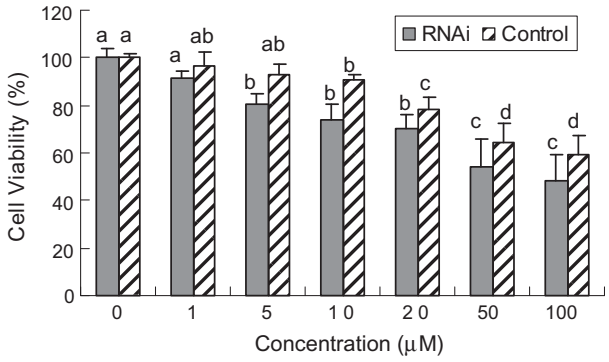

Fig. 4. Cell viability in *Nix* (RNAi) and scrambled (Control) shRNA HEK 293 cells in the response to OTA treatment. The cells were treated with OTA at 0–100 μM for 5 h, followed by WST-8 cell survival assay. Different lowercase letters indicate significant differences ($p < 0.05$). Data were shown in mean ± SD ($n = 5$).

shRNA cells. Altogether, Nix plays a critical role in the OTA-induced autophagy pathway.

4. Discussion

4.1. OTA induces autophagy and mitophagy

Autophagy is responsible for the degradation of toxic protein aggregates and unneeded organelles. Both insufficient and excess

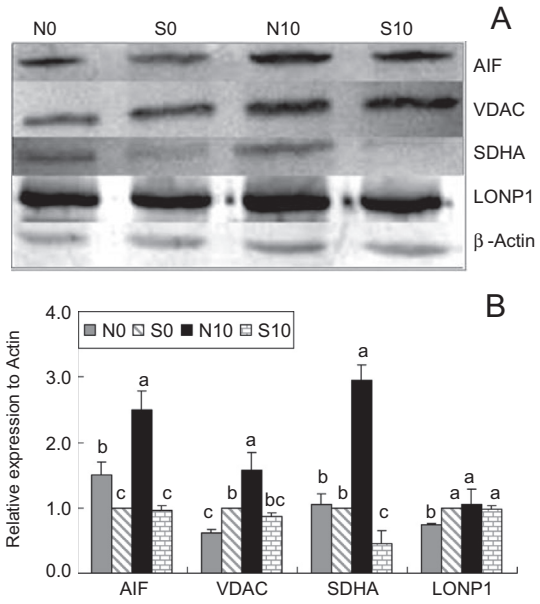

Fig. 6. The expression of selective proteins in *Nix* and scrambled shRNA HEK 293 cells after OTA treatment. Representative blots were shown. Groups are the same as described in Fig. 5. Bars without sharing a common letter differ ($p < 0.05$). Data are means ± SD ($n = 3$).

autophagy seems to be capable of promoting cell injury. Thus, appropriate regulation of autophagy is essential for cellular well-being (Kim et al., 2007). Autophagy can suppress cell death by adaptive responses to various forms of stress (Maiuri et al., 2007). Consistent with this notion, we observed that OTA treatment promotes autophagy during the early development of cytotoxicity (Fig. 1). However, massive autophagy can also kill cells (Maiuri et al., 2007), which is one cause of OTA induced the increase of cell death in our previous experiment (Shen et al., 2013).

Autophagic delivery to lysosomes is the major degradation pathway of mitochondrial turnover, and the term mitophagy refers to mitochondrial degradation by autophagy. Mounting evidence indicates that mitophagy is a selective process (Kim et al., 2007). Therefore, we have assessed mitophagy in OTA-induced cytotoxicity, and the results show that OTA treatment induces an increase in mitophagic flux activity (Fig. 2). This indicates that OTA can induce mitochondrial dysfunction and damage, which is in line with our previous results showing OTA-induced ROS and mitochondrial membrane potential ($\Delta\Psi_m$) changes (Shen et al., 2013).

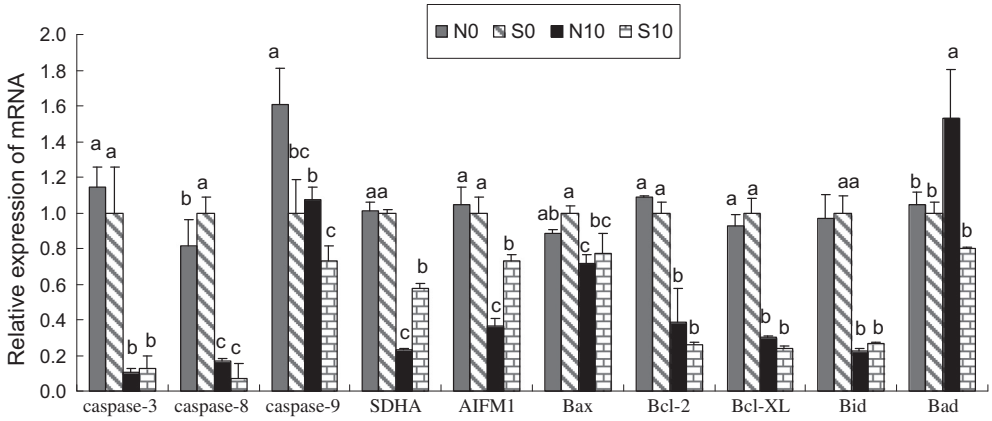

Fig. 5. The mRNA expression of selective genes in *Nix* and scrambled shRNA HEK 293 cells after OTA treatment. The shRNA HEK 293 cells were treated with (1) 0 μM OTA for 5 h in control group (group S0); (2) 0 μM OTA for 5 h in RNAi group (group N0); (3) 10 μM OTA for 5 h in control group (group S10); and (4) 10 μM OTA for 5 h in RNAi group (group N10). Bars without sharing a common letter differ ($p < 0.05$). Data are means ± SD ($n = 3$).

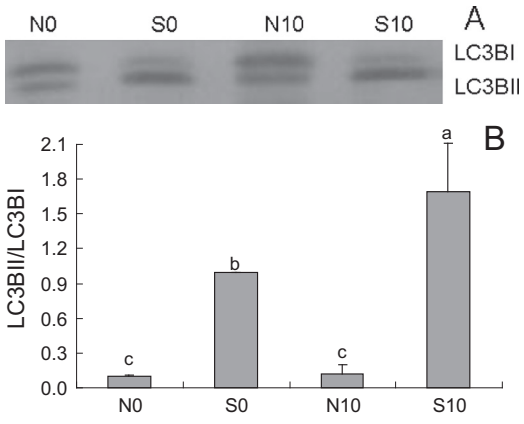

Fig. 7. The ratio of LC3BII/LC3BI in *Nix* and scrambled shRNA HEK 293 cells after OTA treatment. The Nix and scrambled shRNA HEK 293 cells were treated with OTA as described in Fig. 5. Bars without sharing a common letter differ ($p < 0.05$). Data are means ± SD ($n = 3$).

Because *Nix* functions as a regulated mitophagy receptor (Novak, 2012), we employed *Nix* knockdown to determine the role of mitophagy in the mechanisms of the renal cytotoxicity induced by OTA. The results demonstrate that *Nix* knockdown decreases the sensitivity of mitophagy events (Fig. 7) and increases cell death (Fig. 4), indicating that mitophagy plays an important role for cells in the response to OTA-induced renal cytotoxicity.

4.2. OTA disturbes homeostasis between autophagy and apoptosis

The two major apoptosis pathways are the mitochondrial pathway and the death receptor pathway. The mitochondrial pathway is regulated by members of the Bcl-2 protein family, including anti-apoptotic (Bcl-2, Bcl-X_L, Bcl-w, BOO/DIVA, A1/Bfl-1, Mcl-1, NR-13) and pro-apoptotic (Bax, Bak, Bcl-X_S, Bok, Bid, Bad, Bik, Bim, Blk, Hrk, Nix, BNip3, Noxa, PUMA and Bcl-rambo) proteins (Antonsson, 2001). The key players in the death receptor pathway include Fas and tumor necrosis factor. When Fas ligand binds to Fas receptor, the adaptor molecule FADD/Mort-1 is recruited to the receptor, allowing binding and autoactivation of procaspase-8. When caspase-8 is activated, it can process effector caspases (caspase-3, -6, and -7), inducing a cascade of caspase cleavage on their substrates (Bossy-Wetzel and Green, 1999).

The expression of anti-apoptotic genes (*Bcl-2* and *Bcl-X_L*) and pro-apoptotic genes (*Bax* and *Bid*) are significantly suppressed by OTA treatment (Fig. 5), indicating a coordinated response to keep apoptotic death in balance. Furthermore, Nix deficiency does not play a role in the expression of these four apoptosis genes after OTA treatment. In contrast, *Bad* mRNA level was induced by OTA only when Nix expression is deficient (Fig. 5), which might explain the increased sensitivity to OTA in *Nix* shRNA cells (Fig. 4). This result also indicates that selective apoptosis factors can be induced when autophagy is defective by Nix deficiency in the cytotoxic response to OTA. Furthermore, autophagy seems to play an important role to protect against OTA-induced renal cytotoxicity. Although the mechanisms through which autophagy and apoptosis interplay in the response to OTA cytotoxicity are not entirely clear, it is possible that the inhibition of autophagy results in a bioenergetic shortage that triggers apoptosis (Maiuri et al., 2007).

The expression of *caspase-3*, *caspase-8* and *caspase-9* is down-regulated by the treatment of OTA (Fig. 5). Bid is a specific proximal substrate of caspase-8 in the Fas apoptotic signaling pathway. While full-length Bid is localized in cytosol, truncated Bid (tBid) translocates to mitochondria and thus induces the release of cytochrome c from mitochondria (Li et al., 1998). In addition to caspase-8, caspase-3 can also cleave Bid and thus induce cytochrome c release in response to caspase cleavage. Cytosolic cytochrome c binds to Apaf-1, which then permits recruitment of procaspase. Oligomerization results in autoactivation of procaspase-9 (Bossy-Wetzel and Green, 1999). Activated caspase-9 initiates a caspase cascade involving the downstream executioners caspase-3, -6, and -7 (Srinivasula et al., 1998). In the mitochondrial pathway, the complex of cytochrome c, Apaf-1, and caspase-9, called the "apoptosome", is a critical activator of the effector caspases (Bossy-Wetzel and Green, 1999). However, the current model of apoptosis holds that upstream signals lead to activation of downstream effector caspases. Lakhani et al. (2006) conclude that caspases-3 and -7 are critical mediators of mitochondrial events of apoptosis. In the present experiment, the expression of three apoptotic genes (*caspase-3*, *caspase-8*, and *caspase-9*) was inhibited by the treatment of OTA (Fig. 5), which suggest that, in the early stage of OTA-induced renal cytotoxicity, cells respond to OTA by induction of cell survival programs via inhibition of the expression of apoptotic genes. The inhibitor-of-apoptosis (IAP) family of genes has an evolutionarily conserved role in regulating programmed cell death (Deveraux et al., 1997). Human XIAP, c-IAP1, and c-IAP2 can block cytochrome c-induced activation of procaspase-9, thus preventing the activation of caspases-3, -6 and -7. In contrast, these IAPs do not prevent caspase-8-induced proteolytic activation of procaspase-3; however, they subsequently inhibit active caspase-3 directly, thus blocking downstream apoptotic events such as further activation of caspases (Deveraux et al., 1998).

Caspase-9, the essential initiator caspase required for apoptosis signaling through the mitochondrial pathway (Würstle et al., 2012). In the present experiment, Nix knockdown significantly increases the expression of *caspase-9* (Fig. 5), which might suggest that when autophagy is inhibited in Nix deficiency, apoptosis via mitochondrial pathway might be increased.

Nix deficiency and OTA treatment significantly increases the protein expression of AIF (Fig. 6), which might suggest cell death induction (Fig. 4) when the sensitivity of autophagy is inhibited by *Nix* knockdown. This also suggests that autophagy is important for cells to counteract OTA-induced renal cytotoxicity. Interestingly, in *Nix* shRNA cells, the gene expression of *AIFM1* is inhibited by the treatment of OTA. This suggests that the over-expression of AIF provokes a feedback inhibition mechanism to suppress the expression of *AIFM1*.

4.3. OTA disturbs TCA cycle and mETC

There is compelling evidence that VDAC1 may act in the cross-talk between the mitochondria and the cytoplasm by interacting with enzymes involved in energy metabolism and proteins involved in mitochondrial-induced apoptosis (Meins et al., 2008). Cells with low levels of VDAC1 limit metabolite exchange between mitochondria and cytosol (Abu-Hamad et al., 2006). In *Nix* shRNA cells, the protein expression of VDAC1 is up-regulated, and thus the synthesis of ATP increased, explaining why LONP1 is up-regulated in response to OTA treatment (Fig. 6). LONP1 has been shown to selectively recognize and degrade the oxidized, hydrophobic form of aconitase 2 (ACO2) after mild oxidative modification (Bota and Davies, 2002). The up-regulation of LONP1 facilitates the progress of TCA cycle may explain of the OTA-induced SDHA up-regulation (Fig. 6). Moreover, SDHA is known to be a member of mitochondrial electron transport complex II. Under normal circumstances, autophagy can regulate ATP production and homeostasis via nutrient recycling (He and Klionsky, 2009). In present study, autophagic activity was inhibited by *Nix* knockdown, and thus the production of ATP was down-regulated. To deal with this circumstance, the protein expression of VDAC1 was up-regulated followed by the up-regulation of LNOP1 and SDHA in response to

OTA. These promoted the progress of TCA cycle and mitochondrial electron transport chain (mETC). However, VDAC1 expression was slightly down-regulated and SDHA was observably down-regulated in response to OTA, which demonstrated that OTA disturbed TCA cycle and mETC. Therefore, the treatment of OTA is likely to promote autophagy to produce ATP to counteract the perturbation of TCA cycle and mETC. If the production of ATP from autophagy is not sufficient to counteract OTA-induced perturbation of TCA cycle and mETC or autophagy is inhibited, other stress response mechanisms might be provoked, such as the up-regulation of VDAC1 identified herein. All the results might indirectly imply that autophagy may play a critical role in counteracting OTA-induced perturbation of TCA cycle and mETC.

5. Conclusions

Here we demonstrate a central role of Nix in the autophagic response to OTA treatment. To recapitulate, *Nix* shRNA HEK 293 cells are more sensitive than scrambled shRNA cells to OTA-induced cell death, and differentially affect the mRNA expression of *SDHA*, *AIFM1*, and *Bad* and protein expression of AIF, VDAC, SDHA and LONP1after OTA treatment. The gene expression of pro-apoptotic *Bad* and the protein expression of AIF were up-regulated by OTA in *Nix* knockdown cells, which might explain the higher ratio of cell death. These results might indicate that autophagy play a critical role for cells to protect against OTA-induced early renal cytotoxicity. In addition, scrambled but not *Nix* shRNA cells show down-regulation of VDAC1 and SDHA after OTA treatment, suggesting that OTA may disturbe TCA cycle and mETC. It is of future interest to elucidate the link between energy metabolism and autophagy in the Nix regulation on OTA-induced renal cytotoxicity.

Conflict of Interest

The authors declare that there are no conflicts of interest.

Transparency Document

The Transparency document associated with this article can be found in the online version.

Acknowledgements

The paper was supported by the Program for New Century Excellent Talents in University (2014FG046) and ZMKD2013-022. The authors wish to acknowledge Dr. Haoshu Luo and Dr. Chao Wei of China Agricultural University, Dr. Yingcong Li of Institute of Psychology, Chinese Academy of Sciences.

References

Abu-Hamad, S., Sivan, S., Shoshan-Barmatz, V., 2006. The expression level of the voltage-dependent anion channel controls life and death of the cell. Proc. Nat. Acad. Sci. 103, 5787–5792.
Aleo, M.D., Wyatt, R.D., Schnellmann, R.G., 1991. Mitochondrial dysfunction is an early event in ochratoxin a but not oosporein toxicity to rat renal proximal tubules. Toxicol. Appl. Pharmacol. 107, 73–80.
Antonsson, B., 2001. Bax and other pro-apoptotic Bcl-2 family "killer-proteins" and their victim the mitochondrion. Cell Tissue Res. 306, 347–361.
Batlevi, Y., La Spada, A.R., 2011. Mitochondrial autophagy in neural function, neurodegenerative disease, neuron cell death, and aging. Neurobiol. Dis. 43, 46–51.
Bhatnagar, D., Yu, J., Ehrlich, K.C., 2002. Toxins of filamentous fungi. Chem. Immunol. 81, 167–206.
Bossy-Wetzel, E., Green, D.R., 1999. Caspases induce cytochrome C release from mitochondria by activating cytosolic factors. J. Biol. Chem. 274, 17484–17490.
Bota, D.A., Davies, K.J.A., 2002. Lon protease preferentially degrades oxidized mitochondrial aconitase by an ATP-stimulated mechanism. Nat. Cell Biol. 4, 674–680.
Deveraux, Q.L., Takahashi, R., Salvesen, G.S., Reed, J.C., 1997. X-linked IAP is a direct inhibitor of cell-death proteases. Nature 388, 300–304.
Deveraux, Q.L., Roy, N., Stennicke, H.R., Van Arsdale, T., Zhou, Q., Srinivasula, S.M., Alnemri, E.S., Salvesen, G.S., Reed, J.C., 1998. IAPs block apoptotic events induced by caspase-8 and cytochrome c by direct inhibition of distinct caspases. EMBO J. 17, 2215–2223.
Ding, W.X., Ni, H.M., Li, M., Liao, Y., Chen, X., Stolz, D.B., Dorn Ii, G.W., Yin, X.M., 2010. Nix is critical to two distinct phases of mitophagy, reactive oxygen species-mediated autophagy induction and Parkin-ubiquitin-p62-mediated mitochondrial priming. J. Biol. Chem. 285, 27879–27890.
Duarte, S.C., Pena, A., Lino, C.M., 2010. A review on ochratoxin A occurrence and effects of processing of cereal and cereal derived food products. Food Microbiol. 27, 187–198.
Gusdon, A.M., Chu, C.T., 2011. To eat or not to eat: neuronal metabolism, mitophagy, and parkinson's disease. Antioxid. Redox Signal. 14, 1979–1987.
Hald, B., 1991. Porcine nephropathy in Europe. IARC Sci. Publ., 49–56.
He, C., Klionsky, D.J., 2009. Regulation mechanisms and signaling pathways of autophagy. Annu. Rev. Genet. 43, 67–93.
Jin, S., 2006. Autophagy, mitochondrial quality control, and oncogenesis. Autophagy 2, 80–84.
Kanki, T., 2010. Nix, a receptor protein for mitophagy in mammals. Autophagy 6, 433–435.
Kim, I., Rodriguez-Enriquez, S., Lemasters, J.J., 2007. Selective degradation of mitochondria by mitophagy. Arch. Biochem. Biophys. 462, 245–253.
Komatsu, M., Ichimura, Y., 2010. Selective autophagy regulates various cellular functions. Genes Cells 15, 923–933.
Lakhani, S.A., Masud, A., Kuida, K., Porter Jr., G.A., Booth, C.J., Mehal, W.Z., Inayat, I., Flavell, R.A., 2006. Caspases 3 and 7: key mediators of mitochondrial events of apoptosis. Science 311, 847–851.
Lemasters, J.J., 2005. Selective mitochondrial autophagy, or mitophagy, as a targeted defense against oxidative stress, mitochondrial dysfunction, and aging. Rejuv. Res. 8, 3–5.
Levine, B., Kroemer, G., 2008. Autophagy in the pathogenesis of disease. Cell 132, 27–42.
Li, H., Zhu, H., Xu, C.-J., Yuan, J., 1998. Cleavage of BID by Caspase 8 mediates the mitochondrial damage in the Fas pathway of apoptosis. Cell 94, 491–501.
Lim, J., Kim, H.W., Youdim, M.B.H., Choe, K.M., Oh, Y.J., 2011. Binding preference of p62 towards LC3-ll during dopaminergic neurotoxin-induced impairment of autophagic flux. Autophagy 7, 50–59.
Liu, J., Wang, Y., Cui, J., Xing, L., Shen, H., Wu, S., Lian, H., Wang, J., Yan, X., Zhang, X., 2012. Ochratoxin A induces oxidative DNA damage and G1 phase arrest in human peripheral blood mononuclear cells in vitro. Toxicol. Lett. 211, 164–171.
Lühe, A., Hildebrand, H., Bach, U., Dingermann, T., Ahr, H.-J., 2003. A new approach to studying ochratoxin A (OTA)-induced nephrotoxicity: expression profiling in vivo and in vitro employing cDNA microarrays. Toxicol. Sci. 73, 315–328.
Maiuri, M.C., Zalckvar, E., Kimchi, A., Kroemer, G., 2007. Self-eating and self-killing: crosstalk between autophagy and apoptosis. Nat. Rev. Mol. Cell Biol. 8, 741–752.
Marin-Kuan, M., Nestler, S., Verguet, C., Bezencon, C., Piguet, D., Mansourian, R., Holzwarth, J., Grigorov, M., Delatour, T., Mantle, P., 2006. A toxicogenomics approach to identify new plausible epigenetic mechanisms of ochratoxin A carcinogenicity in rat. Toxicol. Sci. 89, 120–134.
Meins, T., Vonrhein, C., Zeth, K., 2008. Crystallization and preliminary X-ray crystallographic studies of human voltage-dependent anion channel isoform I (HVDAC1). Acta Crystall. Sect. F Struct. Biol. Cryst. Commun. 64, 651–655.
Mizushima, N., 2004. Methods for monitoring autophagy. Int. J. Biochem. Cell Biol. 36, 2491–2502.
Mizushima, N., Yamamoto, A., Matsui, M., Yoshimori, T., Ohsumi, Y., 2004. In vivo analysis of autophagy in response to nutrient starvation using transgenic mice expressing a fluorescent autophagosome marker. Mol. Biol. Cell 15, 1101–1111.
Novak, I., 2012. Mitophagy: a complex mechanism of mitochondrial removal. Antioxid. Redox Signal. 17, 794–802.
Novak, I., Kirkin, V., McEwan, D.G., Zhang, J., Wild, P., Rozenknop, A., Rogov, V., Löhr, F., Popovic, D., Occhipinti, A., Reichert, A.S., Terzic, J., Dötsch, V., Ney, P.A., Dikic, I., 2010. Nix is a selective autophagy receptor for mitochondrial clearance. EMBO Rep. 11, 45–51.
O'Brien, E., Dietrich, D.R., 2005. Ochratoxin A: the continuing enigma. Crit. Rev. Toxicol. 35, 33–60.
Rodriguez-Enriquez, S., Kim, I., Currin, R.T., Lemasters, J.J., 2006. Tracker dyes to probe mitochondrial autophagy (mitophagy) in rat hepatocytes. Autophagy 2, 39–46.
Schweers, R., Zhang, J., Randall, M., Loyd, M., Li, W., Dorsey, F., Kundu, M., Opferman, J., Cleveland, J., Miller, J., 2007. NIX is required for programmed mitochondrial clearance during reticulocyte maturation. Proc. Nat. Acad. Sci. 104, 19500–19505.
Shen, X.L., Wu, J.M., Chen, Y., Zhao, G., 2010. Antimicrobial and physical properties of sweet potato starch films incorporated with potassium sorbate or chitosan. Food Hydrocoll. 24, 285–290.
Shen, X.L., Zhang, Y., Xu, W., Liang, R., Zheng, J., Luo, Y., Wang, Y., Huang, K., 2013. An iTRAQ-based mitoproteomics approach for profiling the nephrotoxicity mechanisms of ochratoxin A in HEK 293 cells. J. Proteomics 78, 398–415.
Srinivasula, S.M., Ahmad, M., Fernandes-Alnemri, T., Alnemri, E.S., 1998. Autoactivation of procaspase-9 by Apaf-1-mediated oligomerization. Mol. Cell 1, 949–957.

Stoev, S.D., 1998. The role of ochratoxin A as a possible cause of Balkan endemic nephropathy and its risk evaluation. Vet. Hum. Toxicol. 40, 352–360.
Stoev, S.D., Vitanov, S., Anguelov, G., Petkova-Bocharova, T., Creppy, E.E., 2001. Experimental mycotoxic nephropathy in pigs provoked by a diet containing ochratoxin A and penicillic acid. Vet. Res. Commun. 25, 205–223.
Studer-Rohr, I., Schlatter, J., Dietrich, D.R., 2000. Kinetic parameters and intraindividual fluctuations of ochratoxin A plasma levels in humans. Arch. Toxicol. 74, 499–510.
van der Merwe, K.J., Steyn, P.S., Fourie, L., Scott, D.B., Theron, J.J., 1965. Ochratoxin A, a toxic metabolite produced by *Aspergillus ochraceus* Wilh. Nature 205, 1112–1113.
Vives-Bauza, C., Przedborski, S., 2011. Mitophagy: the latest problem for Parkinson's disease. Trends Mol. Med. 17, 158–165.
Würstle, M.L., Laussmann, M.A., Rehm, M., 2012. The central role of initiator caspase-9 in apoptosis signal transduction and the regulation of its activation and activity on the apoptosome. Exp. Cell Res. 318, 1213–1220.